Atomic Partitioning of Molecular Electrostatic Potentials

D. S. Kosov and P. L. A. Popelier*

Department of Chemistry, UMIST, Manchester, M60 1QD, England

Received: January 27, 2000; In Final Form: May 25, 2000

The theory of atoms in molecules (AIM) defines bounded atomic fragments in real space that generate transferable atomic properties. As part of a program that investigates the topological partitioning of electromagnetic properties based on the electron density, we have calculated the exact atomic electrostatic potential (AEP) of an AIM atom in a molecule. Second we expand this atomic electrostatic potential in terms of AIM electrostatic multipole moments based on spherical tensors. We prove that the convergence of this expansion is faster than previously assumed, even for complicated atomic shapes.

1. Introduction

Progress in the field of molecular electrostatics[1,2] accelerated after the concept of the molecular electrostatic potential (MEP) was introduced.[3] The MEP is a physically observable quantity and can be derived directly from the wave function. The important role the MEP plays in computational chemistry is indicated by its many applications[1] in reactivity (electrostatic catalysis[4]), zeolites[5] (and more generally crystal surfaces and cavities), solvation,[6] complementarity and similarity (encompassing host−guest interactions[7] and structure−activity relationships[8]).

The electrostatic potential has also proved to be very useful in rationalizing the interactions between molecules at large separations and for molecular recognition processes.[9] In particular the role of the electrostatic interaction in proteins cannot be overestimated.[10] The initial step in many biological processes such as drug−receptor or enzyme−substrate interactions is molecular recognition, in which the receptor recognizes key features of the approaching drug. This recognition, which precedes formation of covalent bonds, is believed to occur when two molecules involved in the process are at a relatively large separation. Loosely speaking two molecules first see each other by means of the electrostatic potential.[11]

In this contribution we focus on the atomic partitioning of the MEP within the context of the theory of atoms in molecules (AIM).[12,13] This theory provides a rigorous scheme to cut a molecule into atoms in real space, rather than in the Hilbert space of the basis functions. AIM multipole moments have been used before in the representation of the electrostatic potential[14−16] and of the electrostatic interaction between simple molecules.[17,18]

We introduce the exact AIM *atomic electrostatic potential* (AEP) and the convergence behavior of the AIM electrostatic moments to this AEP. It will be shown that this convergence is attained at lower order than previously assumed.[19,20] We hereby extend the list of useful atomic properties that distribute important molecular quantities over atoms. This list includes a bond order,[21] an atomic valence index,[21] atomic frequency-independent[22] and frequency-dependent[23] polarizabilities, and an atomic dispersion coefficients.[24] All these properties benefit from being independent of the underlying computational scheme that yields the wave function. More precisely, they can be used with Gaussian, Slater, or plane wave functions, are stable with respect to basis set variation,[21,22] and exist within the framework of classic correlation methods, including DFT approaches.

In Section 2 we define the AEP after a concise outline of the construction of an atomic basin Ω. In Section 3 the AEP is expanded in a basis of spherical harmonics introducing electrostatic AIM moments. We rigorously discuss the condition of formal convergence of the AEP in terms of the AIM moments. In Section 4 computational details are given on both the method and the convergence assessment of the AEP. Finally we apply the new AIM concept in Section 5 to a set of molecules including molecular nitrogen, water, ammonia, imidazole, alanine, and valine.

2. Atomic Partitioning of the Exact Molecular Electrostatic Potential

The molecular electrostatic potential (MEP), denoted by $V(\mathbf{r})$, can be computed exactly from the molecular electron density $\rho_{\text{elec}}(\mathbf{r}') = -\rho(\mathbf{r}')$ and the nuclear charge density $\rho_{\text{nuc}}(\mathbf{r}')$, by

$$V(\mathbf{r}) = \int \mathrm{d}\mathbf{r}' \frac{\rho_{\text{tot}}(\mathbf{r}')}{|\mathbf{r} - \mathbf{r}'|} = \int \mathrm{d}\mathbf{r}' \frac{\rho_{\text{nuc}}(\mathbf{r}') + \rho_{\text{elec}}(\mathbf{r}')}{|\mathbf{r} - \mathbf{r}'|} = \sum_A \frac{Z_A}{|\mathbf{r} - \mathbf{R}_A|} - \int \mathrm{d}\mathbf{r}' \frac{\rho(\mathbf{r}')}{|\mathbf{r} - \mathbf{r}'|} \quad (1)$$

where Z_A is the charge of nucleus A located at position $\mathbf{R}_A$, $\mathbf{r}'$ are the three coordinates describing the molecular charge density and $\mathbf{r}$ are the three coordinates describing the MEP. The right-hand side of eq 1 follows from $\rho_{\text{nuc}}(\mathbf{r}') = \sum_A Z_A \delta(\mathbf{r}' - \mathbf{R}_A)$ since in this work the nuclear charge density is represented by monopoles only. It should be noted that the volume integral extends over all space. The MEP has a clear physical meaning because, when multiplied by a unit charge, it is simply the work done of bringing a proton from infinity to the point $\mathbf{r}$. Although $V(\mathbf{r})$ is actually a potential it is often expressed in units of energy, such as kJ/mol, a convention we adopt in this article. An alternative interpretation of MEP is to regard it as the electrostatic interaction energy of a molecule with a proton situated at the point $\mathbf{r}$. In reality this proton induces polarization of the molecular electron density, but this effect is not taken into account here since $\rho(\mathbf{r})$ corresponds to the unperturbed molecular ground state.

* To whom correspondence should be sent. Fax: 44-161-2367677. Tel.: 44-161-2004511. E-mail: pla@umist.ac.uk.

10.1021/jp0003407 CCC: $19.00
Published on Web 07/18/2000

Atomic properties are defined as volume integrals over the atomic basin Ω of a property density. As a consequence of the AIM partitioning a molecule is divided in nonoverlapping atoms, hence a molecular property is simply the sum of the values of the corresponding atomic property. The AEP caused by the electron density of an atom A is given by:

$$V_A(\mathbf{r}) = \frac{Z_A}{|\mathbf{r} - \mathbf{R}_A|} - \int_{\Omega_A} d\mathbf{r}' \frac{\rho(\mathbf{r}')}{|\mathbf{r} - \mathbf{r}'|} \quad (2)$$

where Ω_A is the atomic basin housing nucleus A and the remaining symbols have the same meaning as in eq 1. The total MEP is then merely a sum of all the AEPs, or:

$$V(\mathbf{r}) = \sum_A V_A(\mathbf{r}) = \sum_A \left[\frac{Z_A}{|\mathbf{r} - \mathbf{R}_A|} - \int_{\Omega_A} d\mathbf{r}' \frac{\rho(\mathbf{r}')}{|\mathbf{r} - \mathbf{r}'|} \right] \quad (3)$$

We emphasize that the proposed partitioning occurs in real space consistent with successful and practically useful AIM concepts such as AIM distributed polarizabilities, dispersion coefficients, and bond orders.

There are alternative partitioning schemes for the MEP in Hilbert space, such as distributed multipole analysis (DMA)[25] or a quantum chemical model for electrostatic effects by Jug.[26] These Hilbert space partitioning models have in common that molecular properties are distributed over atoms purely on the basis of the proximity of the centers of the basis functions to the nuclei. As a result, an atomic property is entirely dictated by the positioning of the basis functions contributing to the corresponding molecular property. The AIM partitioning method does not depend on where the basis functions are centered, their mathematical shape, or even whether they exist in the first place, such as in the case of grid determined properties. It assigns in a nontrivial way which portions of real space contribute to a given atom, based on the shape of the interatomic surfaces, which are in turn determined by the *total* electron density.

However, a numerical evaluation of the exact AEP in eq 2 requires an atomic integration for every given point (coordinates $\mathbf{r}$) for which the potential needs to be evaluated. By introducing a Taylor expansion of the integrand $|\mathbf{r} - \mathbf{r}'|^{-1}$ one can separate the electronic coordinates $\mathbf{r}'$ from those describing the electrostatic potential, $\mathbf{r}$. The atomic integration then leads to atomic multipoles, which can subsequently be used to compute the electrostatic potential via the developed series expansion. The advantage of the coordinate separation is clear: the integration does not need to be performed for every given point $\mathbf{r}$ for which one wants to know the potential. The only price paid for this series expansion is possible convergence problems, a matter that is discussed in the next section.

3. Multipole Expansion for Atomic Fragments

It is known that an expansion of the electrostatic potential in terms of Cartesian tensors leads to unwieldy expressions and redundant moments.[27] Hence we follow the route of the spherical tensor formalism. The expression $|\mathbf{r} - \mathbf{r}'|^{-1}$ is conveniently expanded in terms of spherical harmonics,[28] as is shown in eq 4.

$$\frac{1}{|\mathbf{r} - \mathbf{r}'|} = \sum_{l=0}^{\infty} \frac{r_<^l}{r_>^{l+1}} \sum_{m=-l}^{l} (-1)^m C_{l-m}(\theta',\varphi') C_{lm}(\theta,\varphi) \quad (4)$$

In this expression, $r_<$ is the smaller and $r_>$ is the larger value of $r = |\mathbf{r}|$ or $r' = |\mathbf{r}'|$, where both vectors $\mathbf{r}$ and $\mathbf{r}'$ are referred to the same origin. The function $C_{lm}(\theta,\varphi)$ is the renormalized spherical harmonic, denoted by $Y_{lm}(\theta,\varphi)$:

$$C_{lm}(\theta,\varphi) = \sqrt{\frac{4\pi}{2l+1}} Y_{lm}(\theta,\varphi) \quad (5)$$

Below we use this series expansion to expand the AEP rather than the MEP, hence the origin of this series expansion will be taken as the nuclear origin of atom A, not the molecular origin.

Since we compute the electrostatic potential *outside* an electron distribution the radius r' of the electronic coordinate $\mathbf{r}'$ is in principle smaller than the radius r of the potential coordinate $\mathbf{r}$. Thus for our application we will replace $r_<$ by r' and $r_>$ by r in subsequent formulas. For computational convenience we introduce the real functions $C_{lmc}(\theta,\varphi)$ and $C_{lms}(\theta,\varphi)$ by the following unitary transformation:[19]

$$C_{lmc}(\theta,\varphi) = \sqrt{\frac{1}{2}}((-1)^m C_{lm}(\theta,\varphi) + C_{l-m}(\theta,\varphi)) \quad (6a)$$

$$iC_{lms}(\theta,\varphi) = \sqrt{\frac{1}{2}}((-1)^m C_{lm}(\theta,\varphi) - C_{l-m}(\theta,\varphi)) \quad (6b)$$

The multipole expansion (eq 4) can be rewritten in terms of real renormalized spherical harmonics:

$$\frac{1}{|\mathbf{r} - \mathbf{r}'|} = \sum_{l=0}^{\infty} \frac{r'^l}{r^{l+1}} C_{l0}(\theta',\varphi') C_{l0}(\theta,\varphi) + \sum_{l=0}^{\infty} \frac{r'^l}{r^{l+1}} \sum_{m=1}^{l} C_{lmc}(\theta',\varphi') C_{lmc}(\theta,\varphi) + \sum_{l=0}^{\infty} \frac{r'^l}{r^{l+1}} \sum_{m=1}^{l} C_{lms}(\theta',\varphi') C_{lms}(\theta,\varphi) \quad (7)$$

Note that each term of this expansion is real. Substituting eq 7 into the definition of the AEP (eq 2) we arrive at an exact expansion of the AEP in terms of AIM multipole moments in eq 8.

$$V_A(\mathbf{r}) = \sum_{l=0}^{\infty} r^{-l-1} C_{l0}(\theta,\varphi) Q_{l0}(\Omega_A) + \sum_{l=0}^{\infty} r^{-l-1} \sum_{m=1}^{l} C_{lmc}(\theta,\varphi) Q_{lmc}(\Omega_A) + \sum_{l=0}^{\infty} r^{-l-1} \sum_{m=1}^{l} C_{lms}(\theta,\varphi) Q_{lms}(\Omega_A) \quad (8)$$

where $Q_{l0}(\Omega_A)$,$Q_{lmc}(\Omega_A)$ and $Q_{lms}(\Omega_A)$ represent the AIM multipole moments[13]obtained via integration over the atomic basin Ω_A:

$$Q_{l0} = \int_{\Omega_A} d\mathbf{r}' \rho_{\mathrm{tot}}(\mathbf{r}') r'^l C_{l0}(\theta',\varphi'); \quad Q_{lmc} = \int_{\Omega_A} d\mathbf{r}' \rho_{\mathrm{tot}}(\mathbf{r}') r'^l C_{lmc}(\theta',\varphi'); \quad Q_{lms} = \int_{\Omega_A} d\mathbf{r}' \rho_{\mathrm{tot}}(\mathbf{r}') r'^l C_{lms}(\theta',\varphi') \quad (9)$$

If the nuclear charge density just consists of monopoles the function $\rho_{\mathrm{tot}}(\mathbf{r}')$ can be replaced by $-\rho(\mathbf{r}')$ for all multipole moments except Q_{00}, which can be written as

$$Q_{00} = \int_{\Omega_A} d\mathbf{r}'(-\rho(\mathbf{r}')) + Z_A = -N(\Omega_A) + Z_A = q(\Omega_A)$$

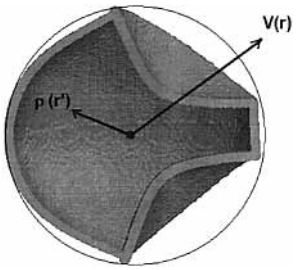

Figure 1. A schematic representation of an atomic basin containing the fragment of the electron density $\rho(\mathbf{r}')$ that generates the corresponding atomic electrostatic potential $V(\mathbf{r})$. Note that $\mathbf{r}'$ and $\mathbf{r}$ have a common origin, i.e., the nucleus of the atom. The circle represents the convergence sphere outside which $V(\mathbf{r})$ *formally* converges.

TABLE 1: Magnitude[a] of the Rank-*l* Multipole Moment, $\bar{Q}_l$ (au), of C_α in Alanine and Upper Limits for Terms, $\bar{Q}_l/R_{conv}^{l+1}$ (kJ/mol), Contributing to the Expansion of the Atomic Electrostatic Potential in eq 8

l	$\bar{Q}_l$ (au)	$\bar{Q}_l/R_{conv}^{l+1}$ (kJ/mol)
0	0.334	143.585
1	0.359	25.320
2	0.426	4.923
3	2.276	4.316
4	2.353	0.731
5	4.227	0.215
6	20.573	0.172
7	51.979	0.071
8	243.368	0.055

[a] The magnitude is computed as $\bar{Q}_l = \sqrt{(Q_{l0})^2+\sum_{m=1}^{l}(Q_{lmc})^2+\sum_{m=1}^{l}(Q_{lms})^2}$ where the moments are defined in eq 9 of the main text.

The main advantage of the multipole expansion is its computational efficiency. As explained in the previous section, the atomic integration is completed *before* the point $\mathbf{r}$ is given at which the AEP needs to be known. Equation 8 makes clear that $V_A(\mathbf{r})$ can be computed at any point using the atomic moments.

We now discuss the issue of the convergence of the multipole expansion of our AEP. Figure 1 shows a schematic representation of an atomic basin containing the electron density $\rho(\mathbf{r}')$ that generates the AEP denoted by $V(\mathbf{r})$. Both vectors $\mathbf{r}'$ and $\mathbf{r}$ are centered on the nuclear origin A. To ensure formal convergence of the multipole expansion we demand that $|\mathbf{r}| > |\mathbf{r}'|$ for all points. This means that a point $\mathbf{r}$ must lie outside a sphere with radius $|\mathbf{r}'|$, where $|\mathbf{r}'|$ is the maximum value encountered within the atomic basin. The atomic basin is bounded, both within the molecule, by the interatomic surfaces, as well as at its open side by a constant electron density envelope. A typical choice is the so-called van der Waals envelope, practically represented by the $\rho = 0.001$ or 0.002 au surface.[29] The AEP will formally diverge for any point $\mathbf{r}$ within the sphere with radius $|\mathbf{r}'|_{max}$ and therefore definitely for any point inside the atomic basin Ω_A. In our calculations we ensured that the potential was evaluated outside the divergence sphere.

This property of formal convergence of the AEP can be considered as an advantage over methods that define multipoles as integrations over whole space. It is well-known that if the whole electron density is included, then the convergence sphere has an infinite radius and the multipole expansion is formally divergent everywhere. Despite this flaw multipole expansion schemes such as DMA[25] are practically useful, presumably because the electron density decays exponentially to zero in the outer regions. Of course, an integration over a finite volume, such as in the computation of the AIM moments, means that some electron density is excluded from the moment. In summary, the practical use of electrostatic moments introduces a tradeoff between exact formal convergence and completeness of the moment. Because of the finiteness of the atomic basins we are able to control convergence, and make it formally exact if necessary.

TABLE 2: Comparison[a] Between the Exact AEP (Calculated by Direct Integration over the Atomic Basin) and the AEP Generated by AIM Moments for a Nitrogen Atom in N_2 and for the Whole Molecule (Sum of AEPs)[b]

	N $R_{conv} = 5.7$		N_2	
l[c]	rms	Δ_{max}	rms	Δ_{max}
0	27.359	42.572	6.348	10.757
1	4.102	7.974	8.006	12.332
2	0.724	2.154	1.020	2.004
3	0.260	0.638	0.477	0.913
4	0.096	0.337	0.147	0.312
5	0.033	0.086	0.053	0.108
6	0.024	0.092	0.040	0.112
7	0.010	0.024	0.016	0.042
8	0.011	0.039	0.016	0.040

[a] Computed for grid points on the water-accessible surface (see text). [b] The root mean square (rms) and absolute value of the maximum deviation (Δ_{max}) are given in kJ/mol, and the convergence radius R_{conv} is given in au. [c] The rank of the multipole, see eq 9.

TABLE 3: Comparison[a] Between the Exact AEP and the AEP Generated by AIM Moments for the Oxygen Atom and the Hydrogen Atom in Water, and for the Whole Molecule (Sum of AEPs)

	O $R_{conv} = 5.08$		H $R_{conv} = 4.15$		H_2O	
l	rms	Δ_{max}	rms	Δ_{max}	rms	Δ_{max}
0	9.657	14.485	8.033	21.276	19.387	27.483
1	3.998	9.845	0.242	1.125	4.079	10.143
2	0.967	2.376	0.211	1.270	1.224	3.695
3	0.440	1.219	0.055	0.313	0.482	1.296
4	0.078	0.195	0.014	0.094	0.086	0.215
5	0.036	0.097	0.014	0.107	0.047	0.194
6	0.032	0.124	0.009	0.037	0.037	0.137
7	0.021	0.059	0.008	0.031	0.027	0.073
8	0.018	0.041	0.008	0.035	0.025	0.066

[a] Specifications identical to those in Table 2.

TABLE 4: Comparison[a] Between the Exact AEP and the AEP Generated by AIM Moments for the Nitrogen Atom and the Hydrogen Atom in Ammonia, and for the Whole Molecule (Sum of AEPs)

	N $R_{conv} = 5.4$		H $R_{conv} = 4.22$		NH_3	
l	rms	Δ_{max}	rms	Δ_{max}	rms	Δ_{max}
0	10.965	21.204	6.967	19.330	5.289	9.590
1	6.959	12.127	0.618	3.878	7.735	14.032
2	1.745	4.924	0.252	1.568	2.130	5.431
3	0.440	1.317	0.029	0.143	0.472	1.438
4	0.089	0.274	0.026	0.252	0.119	0.528
5	0.074	0.245	0.013	0.092	0.084	0.304
6	0.038	0.186	0.008	0.051	0.042	0.225
7	0.013	0.055	0.008	0.050	0.020	0.089
8	0.011	0.042	0.008	0.024	0.018	0.068

[a] Specifications identical to those in Table 2.

4. Computational Methods

In all our calculations the electron density $\rho(\mathbf{r})$ was obtained from the solution of the Kohn−Sham equation. This method is computationally less demanding than the Hartree−Fock/MP2 method but yields comparable results for molecular proper-

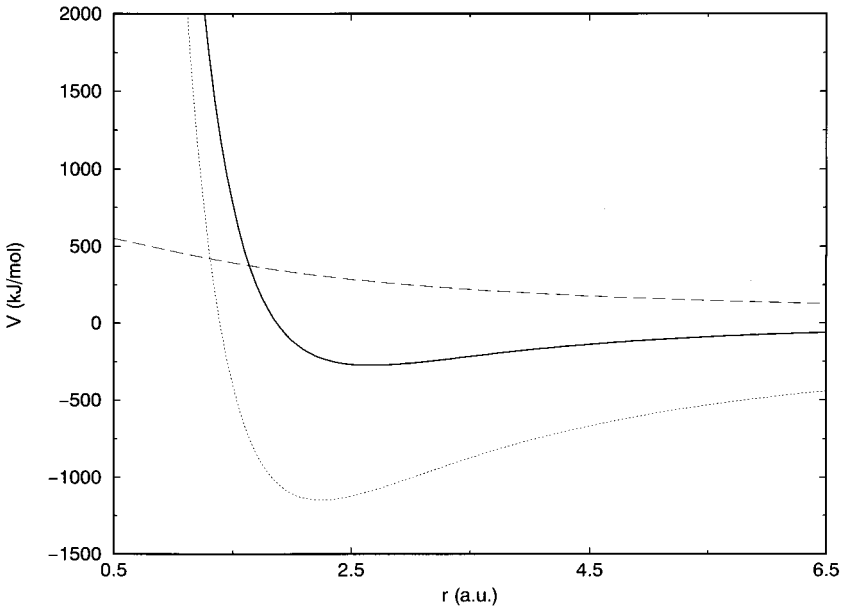

Figure 2. A 1D profile of atomic electrostatic potentials (AEP) along the C_3 symmetry axis in ammonia. Given a test charge of +1 au the potential is expressed in kJ/mol, and the distance r is measured from the nitrogen nucleus. The AEP due to nitrogen (dotted) is added to the AEP of three times the AEP of a single hydrogen (dashed) to yield the MEP (solid). The minimum in the MEP (−272.9 kJ/mol) occurs at 2.7 au, just below a van der Waals surface determined by a typical hard sphere radius of 1.5 Å (or 2.85 au).

TABLE 5: Comparison[a] Between the Exact AEP and the AEP Generated by AIM Moments for All the Atoms in Imidazole and for the Whole Molecule ($C_3N_2H_4$) (Sum of AEPs)

	0		2		4		6	
l	rms	Δ_{max}	rms	Δ_{max}	rms	Δ_{max}	rms	Δ_{max}
C1 (R_{conv} = 5.49)	16.294	38.059	0.696	2.980	0.051	0.214	0.010	0.045
C2 (R_{conv} = 5.46)	12.286	28.410	0.594	2.711	0.049	0.208	0.010	0.042
N3 (R_{conv} = 5.44)	4.323	10.310	0.476	1.692	0.043	0.200	0.008	0.030
C4 (R_{conv} = 5.47)	16.524	35.881	0.567	2.392	0.033	0.147	0.009	0.040
N5 (R_{conv} = 5.46)	4.949	15.452	0.385	1.770	0.053	0.235	0.011	0.045
H6 (R_{conv} = 4.52)	3.826	10.936	0.174	1.033	0.030	0.292	0.011	0.105
H7 (R_{conv} = 4.15)	3.790	11.323	0.179	1.032	0.030	0.286	0.011	0.103
H8 (R_{conv} = 3.70)	5.079	20.215	0.197	1.708	0.022	0.283	0.008	0.040
H9 (R_{conv} = 4.18)	3.815	10.949	0.189	1.172	0.033	0.331	0.011	0.123
$C_3N_2H_4$	19.993	56.090	1.465	4.647	0.171	0.924	0.033	0.162

[a] Specifications identical to those in Table 2.

ties.[30,31] Of the available exchange-correlation functionals, the gradient-corrected hybrid functionals provide the best overall coherence with MP2 theory and experimental data. The B3LYP parametrization, i.e., Becke's three-parameter formulation of the exchange functional[32] and a gradient-corrected correlation functional of Lee, Yang, and Parr[33] have proven to be of reliable quality. The geometry optimizations, wave functions, and MEPs were generated by the program GAUSSIAN94[34] at the B3LYP/6-311+G(2d,p)//HF/6-31G(d,p) level. Although we generated the electrostatic potentials using a fairly high level of theory it has been stated before[9] that varying the level does not greatly affect the overall pattern of the potential for a given molecule. The AIM moments were implemented in MORPHY01[35] up to an arbitrary rank l, high enough to assess the multipole convergence rate thoroughly, as shown in the tables below. The program MORPHY01 also computes the AEP for a given atom directly via eq 2. Since the AEP needs to be known in thousands of points it was implemented efficiently, each point **r** appearing as a parameter inside the inner integration quadrature loop.

The accuracy of the AEP was checked against the MEP, independently computed by GAUSSIAN94 via eq 3. Indeed, the MEP should equal the sum of the AEPs of all atoms in the molecules. For that purpose the root-mean-square (rms) deviation between the MEP and the sum of the AEPs was computed for the order of 10 thousand points lying on the molecular surface, defined by the $\rho = 0.002$ au envelope. The rms deviation amounts to 0.1−0.5 kJ/mol for several test molecules such as water and N_2. This good agreement demonstrates the computational accuracy of the numerical algorithm implemented in MORPHY.[36,37] Furthermore these calculations provide an independent assessment of the error inherent in AIM multipole moments via a physical and measurable quantity, namely the electrostatic potential.

To estimate the convergence rate of the AIM moments we calculated the AEP on the so-called water-accessible surface. This is an important surface from a practical point of view because it indicates the closest approach of a water molecule. Hence in molecular dynamics simulations the electrostatic potential is typically sampled on this surface.[38] We represented the water-accessible surface by 10^4 to 3×10^4 grid points on an envelope lying 1.4−1.5 Å outside the molecular surface. The water-accessible surface was represented by a single envelope of constant electron density, in line with the representation of the molecular surface. This surface is also determined by a single isodensity envelope, usually of $\rho = 0.002$ au. The value of ρ to represent the water-accessible surface was first guessed and then adjusted such that the average distance between the molecular surface and the water-accessible surface was about 1.4 Å. The

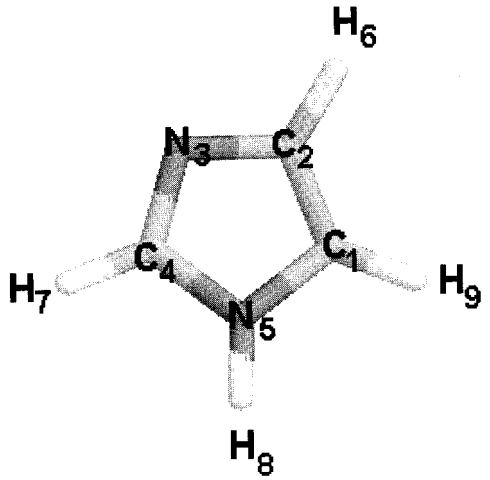

Figure 3. Labeling scheme of imidazole used in Table 5.

water-accessible electron density envelope is typically of the order of $\rho = 10^{-5}-10^{-4}$ au. The AIM electrostatic moments were computed via integration (see eq 9) where the atomic basin was capped by the isodensity envelope of $\rho = 5 \times 10^{-5}-10^{-3}$ au depending on the convergence radius.

It is convenient to visualize the comparison between the exact and multipole generated AEP via the program RasMol.[39] Such visualization contains detailed information complementary to the tables listing the values of the rms and magnitude of the maximum deviations (Δ_{max}). The program RasMol was also used to show a color-coded map of the AEP.

5. Applications and Discussion

We have performed calculations on molecular nitrogen, water, ammonia, imidazole, alanine, and valine, which we will now discuss in turn. Table 1 provides a qualitative assessment of the convergence of the multipole expansion for the C_α in alanine. The magnitudes of the terms in eq 8 can be estimated from the (coordinate-invariant) magnitudes $\bar{Q}_l$ of the multipole moments divided by the appropriate power of the convergence radius R_{conv}. Since $|C_{lm}(\theta,\varphi)| \leq 1$ the term $\bar{Q}_l/R_{conv}^{l+1}$ is an upper limit for the actual contribution to the AEP.

The first test of the usefulness of AIM moments is the generation of AEP for a nitrogen atom in N_2. It is clear from Table 2 that rms deviations of less than 0.1 kJ/mol occur for a nitrogen AEP generated by AIM moments up to rank $l = 4$ (hexadecapole). The multipole-generated MEP computed from the sum of the two nitrogen AEPs yields deviations of less than 0.1 kJ/mol from rank $l = 5$ onward. An early study by Stone and Alderton[40] expected that a nonspherical slice cut off would give rise to a poorly converging multipole series expansion for the total molecule's electrostatic potential. This conjecture, based only on inspection of the magnitude of AIM moments, proves to be wrong. Based on this simple experiment and on further results discussed below we confirm[41] that our form of distributed multipole analysis, which rests on a physical division of space into disjoint regions, is useful. A reduction of the rank invariably leads to additional sites at which multipoles with lower rank are centered, that are obtained via a fitting procedure. We believe that an expansion that only involves nuclear centers is a good

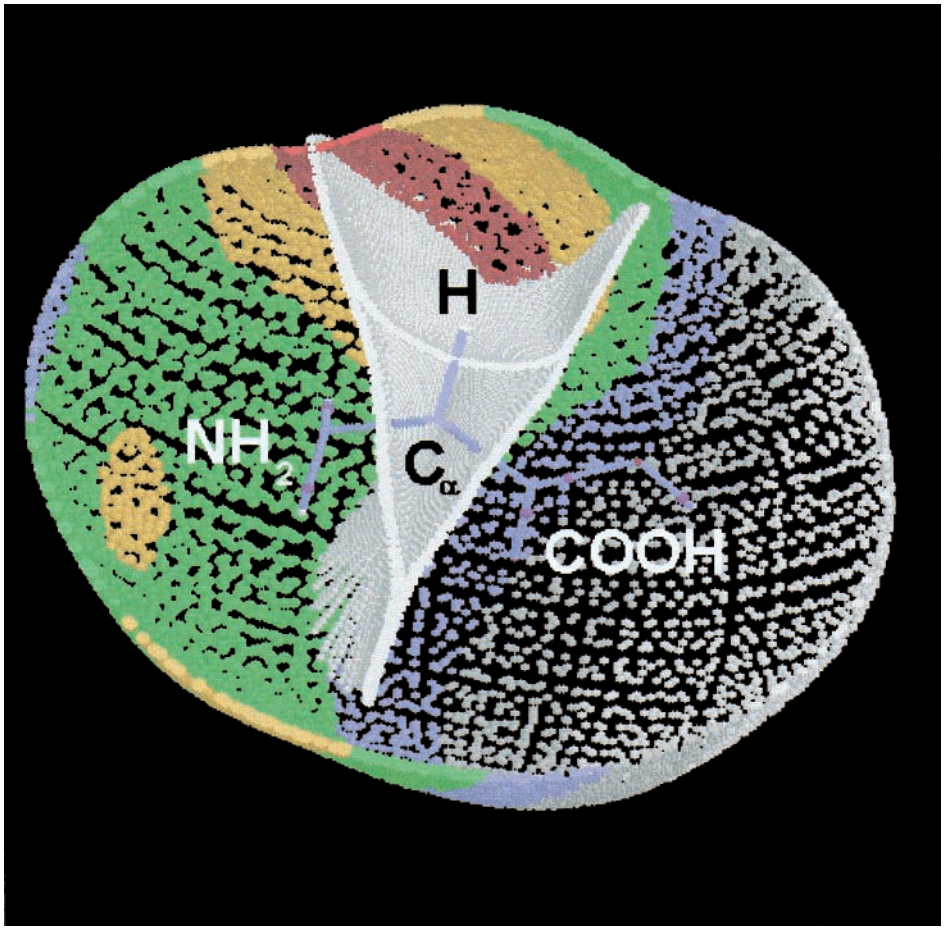

Figure 4. The atomic electrostatic potential (AEP) of C_α on the water-accessible surface around alanine. The part of the picture before the plotting plane has been deleted (slab mode) in order to show the interior of the object. The C_α atom contributes everywhere positively to the molecular electrostatic potential. The most positive region develops near the hydrogen attached to the C_α and protrudes toward to the NH_2 terminus. Color code (in kJ/mol): 81 < white < 91 < gray < 101 < blue < 112 < green < 122 < yellow < 132 < red < 142.

TABLE 6: Comparison[a] Between the Exact AEP and the AEP Generated by AIM Moments for the C_α Atoms in Alanine and Valine

	C_α in alanine $R_{conv} = 6.1$		C_α in valine $R_{conv} = 6.2$	
l	rms	Δ_{max}	rms	Δ_{max}
0	7.791	19.790	7.706	15.534
1	1.459	5.902	0.957	3.043
2	0.827	2.906	0.676	2.052
3	0.121	0.448	0.110	0.372
4	0.025	0.148	0.020	0.104
5	0.020	0.110	0.014	0.083
6	0.010	0.048	0.009	0.042
7	0.008	0.027	0.008	0.026
8	0.008	0.019	0.008	0.017

[a] Specifications identical to those in Table 2.

compromise between the completely inadequate one-center multipole expansion and a practical scheme with fitted low rank multipoles.

Similarly, Table 3 shows that a multipole expansion with multipoles of rank $l > 3$ yields a rms value of less than 0.1 kJ/mol. This limit is reached sooner for hydrogen, namely when $l > 2$. The right columns in Table 3 show the discrepancy for the whole molecule, where the AEPs have been summed over all atoms in the molecule. The hydrogen in ammonia shows similar rapid convergence behavior (Table 4) although the nitrogen atom is slightly slower than the oxygen in water. The nitrogen atom has an rms value of 0.13 kJ/mol when the expansion is truncated at rank four.

We consider the case of ammonia to speculate on an interesting issue that has arisen in connection with a rigorous study on the electrostatic potential $V(r)$ of free atoms. By means of a rigorous derivation starting with Poisson's equation Sen and Politzer proved[41] that $V(r)$ of neutral free spherical atoms is always positive. For negatively charged ions $V(r)$ is initially positive, then it goes through a negative minimum and approaches zero through negative values as $r \rightarrow \infty$. The consequence of this statement for atoms in molecules is intriguing, although it is not known whether it can be generalized to nonspherical atoms.

Figure 2 shows the AEP of nitrogen and the hydrogens in ammonia along the C_3 symmetry axis, as well as their sum resulting in ammonia's MEP. A minimum occurs in the MEP at a distance of 2.7 au from the nitrogen nucleus, just below a typical van der Waals radius of 2.8 au. It is clear that, using the AIM partitioning, this minimum is entirely due to the AEP of the nitrogen atom. It is tempting to relate the existence of this minimum to the negative sign of the nitrogen charge ($q(N) = -0.989$ au) via a possible generalization of Sen and Politzer's findings.[41]

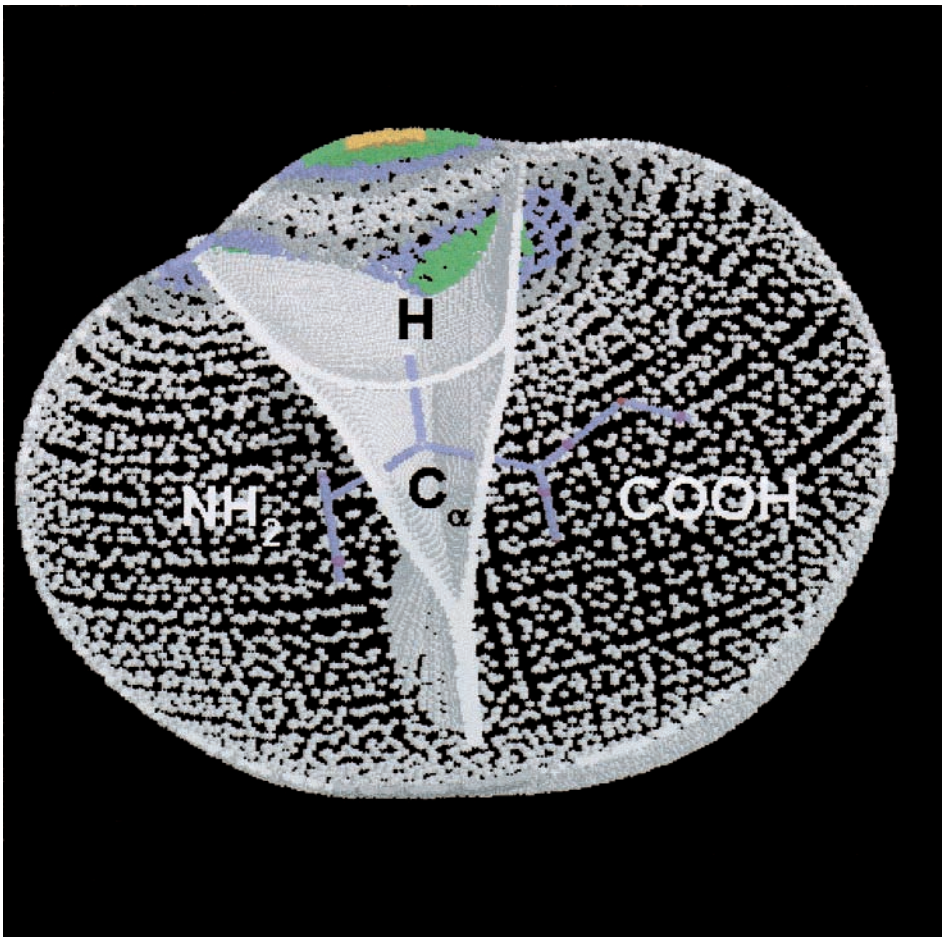

Figure 5. The deviations in the exact AEP and the AEP obtained from the multipole moments up to the octupole ($l = 3$) for the C_α atoms in alanine. The part of the picture in front of the plotting plane is deleted in order to show the interior of the object. The largest deviations occur near the cusplike edges of the atom and the region of closest proximity. Color code (in kJ/mol): white < 0.1 < gray < 0.2 < blue < 0.3 < green < 0.4 < yellow < 0.5. The deviations in the exact AEP and the AEP obtained from the multipole moments up to the octupole ($l = 3$) for the C_α atoms in alanine. The part of the picture in front of the plotting plane is deleted in order to show the interior of the object. The largest deviations occur near the cusplike edges of the atom and the region of closest proximity. Color code (in kJ/mol): white < 0.1 < gray < 0.2 < blue < 0.3 < green < 0.4 < yellow < 0.5.

We have shown the convergence for a simple π system (N_2) and two lone-pair systems (H_2O and NH_3). A further convergence test is provided by an aromatic system, i.e., imidazole. Table 5 (labeling scheme in Figure 3) shows how each atom is converging with increasing multipole rank l. Again most nonhydrogen atoms have reached a rms value of less than 0.1 kJ/mol when $l = 4$, and the hydrogen atoms already have reached it after $l = 2$. We observe that the rms does not always decrease monotonically with increasing l.

With an eye on future applications in the chemistry of peptides we looked at the AEP of the alpha carbon (C_α) atom in alanine and valine. We have visualized the AEP of C_α in alanine in Figure 4. The AEP of the alpha carbon provides only positive contributions to the MEP, with the most positive region (>140 kJ/mol) near the hydrogen atom attached to it, and spreading out toward the NH_2 terminus.

Table 6 again reveals excellent convergence behavior for both C_α atoms where a rms discrepancy of just above 0.1 kJ/mol is seen already for the octupole ($l = 3$). Figure 5 displays the convergence information in more detail than can be seen from a list of rms and Δ_{max} values. For each grid point on the water-accessible surface a color is assigned that marks the deviation between the exact AEP and the AEP generated by the monopole, dipole, quadrupole, and octupole moment.

Figure 5 shows that the atomic electrostatic potential obtained from the multipole expansion differs in the cusp regions, i.e., where the atom extends via long narrow tails. The largest deviations (order 0.5 kJ/mol) occur near the cusplike edges of the atom and the region of closest proximity.

Finally we should comment on the meaning of the atomic population, hence the atomic charge. It is clear from Table 2 that the AEP of a nitrogen atom is poorly represented by the monopole only. Indeed, by symmetry the nitrogen in N_2 must have a vanishing net charge, hence the poor convergence. Instead of shifting the position of this monopole or changing its value in order to fit the potential, we accept that higher multipoles are required to improve the convergence.

6. Conclusions

In this work we have computed for the first time the exact electrostatic potential generated by an AIM atomic fragment, called the AEP. An early study[14] showed plots of a low-order Cartesian multipole expansion, but the current study supersedes this work with a higher-order spherical tensor multipole expansion. The assumption[19,20,40] that the multipole expansion associated with bounded fragments in real space, such as AIM atoms, has poor convergence proves to be wrong. In summary, this study demonstrates that we do not need an excessively large number of multipoles to reproduce the exact ab initio molecular electrostatic potentials within the AIM theory. We can therefore safely add the AEP to the list of practically useful topologically partitioned electromagnetic properties, such as the polarizability and dispersion coefficients.

This work makes clear that the atomic population (or rank-zero multipole moment) is just one term of the expansion of a physically observable quantity, namely the electrostatic potential. Hence the AIM populations (and thus charges) cannot be judged on their reproduction of the electrostatic potential. Instead, they must be seen in the context of a multipole expansion of the AEP.

Acknowledgment. We thank S. E. O'Brien and F. M. Aicken for help in generating wave functions. One of us (D.S.K.) appreciates a valuable discussion with Dr. A. J. Stone. Gratitude is expressed to EPSRC which sponsors this work via grant GR/M18119.

References and Notes

(1) Naray-Szabo, G.; Ferenczy, G. *Chem. Rev.* **1995**, *95*, 829.

(2) Price, S. L. In *Molecular Interactions: From van der Waals to Strongly Bound Complexes*; Scheiner, S., Ed.; John Wiley: Chichester, U.K., 1997.

(3) Scrocco, E.; Tomasi, J. *Fortschr. Chem. Forsch.* **1973**, *42*, 95.

(4) Jiao, H.; Schleyer, P. v. R. *J. Chem. Soc., Faraday Trans.* **1994**, *90*, 1559.

(5) White, J. C.; Hess, C. A. *J. Phys. Chem.* **1993**, *97*, 6398.

(6) Warshel, A.; Aquist, J. *Ann. Rev. Biophys. Chem.* **1991**, *29*, 267.

(7) Sharp, K. A.; Honig, B.; Harvey, S. C. *Biochemistry* **1990**, *29*, 340.

(8) Kenny, P. W. *J. Chem. Soc., Perkin Trans. 2* **1994**, 199.

(9) Murray, J. S., P. Politzer; Sapse, A.-M., Eds.; Oxford University Press: Oxford, U.K., 1998; pp 49−84.

(10) Nakamura, H. *Quarterly Rev. Biophys.* **1996**, *29*, 1.

(11) Naray-Szabo, G. In *Encyclopedia of Computational Chemistry*; Schleyer, P. v. R., Ed.; Wiley: 1998; Vol. 2, p 905.

(12) Bader, R. F. W. *Atoms in Molecules: A Quantum Theory*; Clarendon Press: Oxford, U.K., 1990.

(13) Popelier, P. L. A. *Atoms in Molecules. An Introduction.*; Pearson Education: Harlow, U.K., 1999.

(14) Bader, R. F. W.; Popelier, P. L. A.; Chang, C. *J. Mol. Struct. (THEOCHEM)* **1992**, *255*, 145.

(15) Wiberg, K. B.; Rablen, P. R. *J. Comput. Chem.* **1993**, *14*, 1504.

(16) Breneman, C. M., Thompson, T. R.; Rhem, M.; Dung, M. *Comput. Chem.* **1995**, *19*, 161.

(17) Cooper, D. L.; Stutchbury, N. J. C. *Chem. Phys. Lett.* **1985**, *120*, 167.

(18) Popelier, P. L. A. *Mol. Phys.* **1996**, *87*, 1169−1187.

(19) Stone, A. J. *The Theory of Intermolecular Forces*; Clarendon: Oxford, U.K., 1996.

(20) Chipot, C.; Angyan, J. G.; Millot, C. *Mol. Phys.* **1998**, *94*, 881.

(21) Angyan, J. G.; Loos, M.; Mayer, I. *J. Phys. Chem.* **1994**, *98*, 5244.

(22) Angyan, J. G.; Jansen, G.; Loos, M. C. H.; Hess, B. A. *Chem. Phys. Lett.* **1994**, *219*, 267.

(23) Haettig, C.; Jansen, G.; Hess, B. A.; Angyan, J. G. *Can. J. Chem.* **1996**, *74*, 976.

(24) Haettig, C.; Jansen, G.; Hess, B. A.; Angyan, J. G. *Mol. Phys.* **1997**, *91*, 145.

(25) Stone, A. J. *Chem. Phys. Lett.* **1981**, *83*, 233−239.

(26) Jug, K.; Gerwens, H. *J. Phys. Chem. B* **1998**, *102*, 5217.

(27) Laidig, K. E. *J. Phys. Chem.* **1993**, *97*, 12 760−12 767.

(28) Varshalovich, D. A.; Moskalev, A. N.; Khersonskii, V. K. *Theory of Angular Momentum*; World Scientific: River Edge, NJ, 1988.

(29) Bader, R. F. W.; Carroll, M. T.; Cheeseman, J. R.; Chang, C. *J. Am. Chem. Soc.* **1987**, *109*, 7968.

(30) Bartolotti, L. J.; Flurchick, K. In *Review in Computational Chemistry*; Lipkowitz, K. B., Boyd, D. B., Eds.; VCH: New York, 1996; Vol. 7, p 187.

(31) Wesolowski, T. A.; Weber, J.; Sapse, A.-M., Eds.; Oxford University Press: Oxford, 1998; pp 85−132.

(32) Becke, A. D. *Phys. Rev.* **1988**, *A38*, 3098.

(33) Lee, C.; Yang, W.; Parr, R. G. *Phys. Rev.* **1988**, *B37*, 785.

(34) GAUSSIAN94 M. J. Frisch, G. W. Trucks, H. B. Schlegel, P. M. W. Gill, B. G. Johnson, M. A. Robb, J. R. Cheeseman, T. Keith, G. A. Petersson, J. A. Montgomery, K. Raghavachari, M. A. Al-Laham, V. G. Zakrzewski, J. V. Ortiz, J. B. Foresman, J. Cioslowski, B. B. Stefanov, A. Nanayakkara, M. Challacombe, C. Y. Peng, P. Y. Ayala, W. Chen, M. W. Wong, J. L. Andres, E. S. Replogle, R. Gomperts, R. L. Martin, D. J. Fox, J. S. Binkley, D. J. Defrees, J. Baker, J. P. Stewart, M. Head-Gordon, C. Gonzalez, and J. A. Pople, Gaussian, Inc., Pittsburgh, PA, 1995.

(35) Morphy01 a program written by P. L. A. Popelier with a contribution from R. G. A. Bone, D. Kosov, M. in het Panhuis, UMIST, Manchester, England, EU 2001.

(36) Popelier, P. L. A. *Comp. Phys. Commun.* **1996**, *93*, 212.

(37) Popelier, P. L. A. *Comp. Phys. Commun.* **1998**, *108*, 180.

(38) Leach, A. R. *Molecular Modelling. Principles and Applications*; Longman: Harlow, U.K., 1996.

(39) R.Sayle, RasMol, a molecular visualization program, Glaxo-Wellcome, Stevenage, U.K., 1994.

(40) Stone, A. J.; Alderton, M. *Mol. Phys.* **1985**, *56*, 1047.

(41) Sen, K. D.; Politzer, P. *J. Chem. Phys.* **1989**, *90*, 4370. .